S. A. Prahl, W. F. Cheong, G. Yoon, A. J. Welch, "Optical properties of human aorta during low power argon laser irradiation," in *SPIE Proceedings of Laser Interaction with Tissue*, **908**, pp. 29–33, (1988).

# Optical properties of human aorta during low power argon laser irradiation

Scott A. Prahl, Wai Fung Cheong, Gilwon Yoon, A. J. Welch

University of Texas, Department of Biomedical Engineering
Engineering Science 610, Austin, Texas 78712

## ABSTRACT

The optical properties of human aorta were measured during low power argon laser irradiation ($\sim$100 mW/mm$^2$). The delta-Eddington optical model was iterated to determine the optical properties. The results indicated that the transport albedo was nearly constant ($\sim$0.96) until the onset of tissue charring, after which it decreased quickly. The optical depth gradually declined (after an abrupt initial increase) until tissue charring when it dropped sharply. The anisotropy dropped initially and increased linearly with time of exposure.

## INTRODUCTION

The thermal response of tissue during laser irradiation is highly dependent upon the optical properties of the tissue. The rate of heat generation in tissue can be determined knowing the light distribution and tissue absorption coefficient. This light distribution depends on the optical properties of the tissue. Thermal models assume that the optical properties remain constant during laser irradiation. The thermal models typically produce temperatures substantially above normal tissue temperatures (50–300°C). At such temperatures, dehydration, protein denaturation, coagulation, charring, pyrolysis or ablation may occur. Any of these processes will change the appearance of the tissue (and hence the optical properties of the tissue), and consequently, the light distribution in the tissue. Heretofore, there has been no attempt to measure the optical properties of tissue during irradiation.

## METHOD

The experimental apparatus shown at right was used to measure the scattered transmittance, the scattered reflectance, and the primary transmittance during irradiation of human aorta by an argon laser. Reflectance and transmittance were measured during irradiation, digitized and saved on a computer for later analysis. The laser used was a 20 W argon laser (Coherent CR-18) operating in the multi-line mode. Two integrating spheres were used to measure scattered light. The larger sphere (24 cm in diameter) was used to measure scattered transmittance (Labsphere) and the smaller (12 cm) was used to measure scattered reflectance. Primary transmittance was measured with a 4 mm diameter photodiode located 170 cm from the exit port of the larger integrating sphere. The detectors used to measure light in the integrating sphere were also photodiodes (RCA SK2031). Conversion of reflectance and transmittance measurements into optical properties requires uniform collimated irradiance (because the method is one-dimensional). Consequently, the laser beam was expanded with a 5× microscope objective (f26.4 mm) and collimated with an f126 mm convex lens. The beam was magnified by a factor of 4.8. The outer fringes of the beam were blocked with a circular aperture 8 mm in diameter, thereby allowing only the central "flat" portion of the Gaussian beam profile to reach the sample.

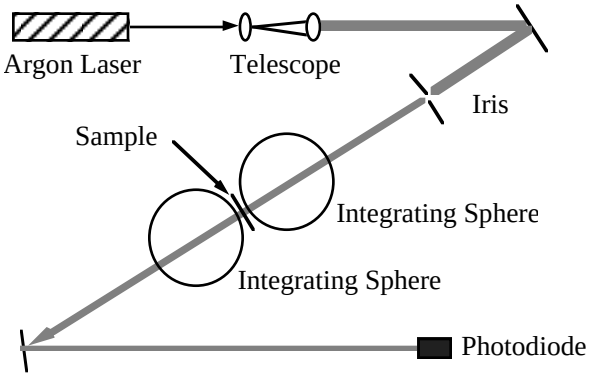


Figure 1: Experimental apparatus.

Aorta was obtained from the morgue the morning the experiments were done. The aorta was kept in chilled saline until used. The adventitia was removed leaving samples with full thickness media and the intact intima. Typical sample thicknesses were about 1.5 mm. The aorta was not sandwiched between glass slides. This allowed the tissue to change shape during irradiation. Typically the samples grew thinner during irradiation due to dehydration. Both experiments reported in this paper use aorta samples from the same subject.

## MEASUREMENTS

During irradiation the tissue passed through a series of phases. The first phase, coagulation, was marked by whitening of the tissue. This was followed by dehydration, by boiling and finally by charring. Before each experiment, measurements of 0% and 100% scattered transmittance, primary transmittance and scattered reflectance were made to allow scaling of detector voltages into fractions of the total possible reflectance or transmittance. These values are plotted in Figure 2 for two experiments with differing irradiances: 130 and 90 $\mathrm{mW/mm^2}$. As expected, reflectance and transmittance change more quickly for the higher irradiance. The tissue response for irradiances between 130 and 90 $\mathrm{mW/mm^2}$ was similar and, for clarity, is not shown.

The difference in magnitude illustrated by the scattered and primary transmittance plots at the right is caused by differing sample thicknesses. (1.65 mm for the higher irradiance and 1.70 mm for the other.) Since one mean free path (mfp) is about 0.1 mm, this is a significant thickness change. This difference is not as evident in the reflectance graph because the samples are so thick (∼15 mfps) that thickness variations do not affect the net reflectance very much.

Both the primary and the scattered transmittance drop substantially in the first 50–75 seconds. Presumably this is due to surface coagulation and dehydration. The initial drop in transmittance is followed by an increase in transmittance caused by subsurface vapor production. Once the vapor pressure exceeds the yielding point of the tissue the bubble of vapor explodes, announced by an audible "pop." This point is indicated at the right by the first dashed and the first dotted lines. The dashed line at the right corresponds to the time of the explosion in 130 $\mathrm{mW/mm^2}$ experiment. The dotted line is for the 90 $\mathrm{mW/mm^2}$ experiment. Note that in the lower irradiance case there is an anomalous early "pop" near the second dashed line. This may have been due to a small plaque deposit.

The onset of charring is marked by a sudden decrease in the reflectance. This is indicated by the second dashed line for the higher irradiance and the second dotted line for the lower irradiance. Not surprisingly, as the tissue blackens during charring, the transmittances also drop.

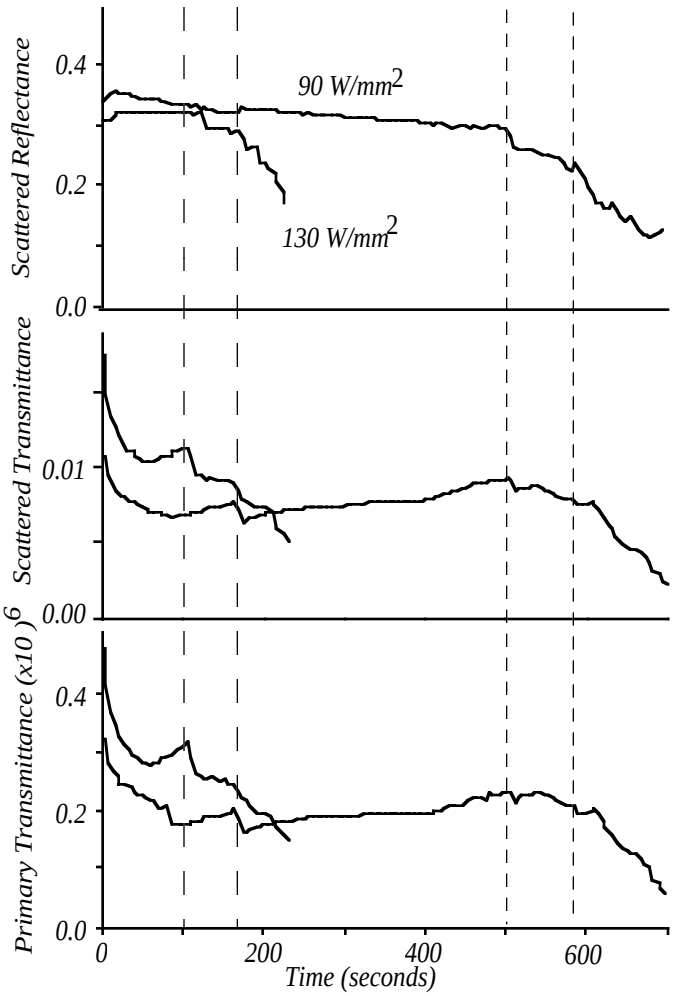


Figure 2: Reflectance and Transmittance

Halldórsson *et al.* have made a similar types of measurements using a Nd-YAG laser on canine stomach wall[1]. They used much higher power densities, smaller spot sizes and shorter irradiation times. They found that the reflectance initially increased and the transmittance decreased. This was followed by a rapid increase in reflectance and continued decrease in transmittance during the evaporation or dehydration phase. Finally, during the carbonization phase they reported that the reflectance decreased and the transmittance increased. Clearly, these results differ from those reported here. This discrepancy is most likely caused by the greater penetration depth of Nd-YAG (1060 nm) light in tissue. This difference causes a change in the light distribution, and consequently, in the thermal profile and the damage pattern for the tissue.

## DATA REDUCTION

The method used to convert reflectance and transmittance measurement to optical properties is based on the delta-Eddington model. This is essentially the P1-approximation of the radiative transport equation using a slightly different phase function, namely

$$P_{\mathrm{delta-Eddington}}(\cos\theta) = \frac{1}{4\pi}\left\{2f\delta(1-\cos\theta) + (1-f)(1+3g'\cos\theta)\right\} \tag{1}$$

This phase function allows reduction of the integro-differential transport equation into a simpler diffusion equation. The diffusion equation has a closed-form solution. This solution yields accurate values for reflectance and transmittance for all materials, including those that are highly forward scattering[2]. This is important since tissue is highly anisotropic[3, 4].

Recent work by Jacques, Alter and Prahl has shown that a modified Henyey-Greenstein function describes volumetric light scattering in human dermis quite well[3]. More recently Yoon *et al.* have found similar results for human aorta at 632 nm[4]. The modified Henyey-Greenstein phase function is

$$P_{\mathrm{modified-HG}}(\cos\theta) = \frac{1}{4\pi}\left\{\beta + (1-\beta)\frac{1-g_0^2}{(1+g_0^2-2g_0\cos\theta)^{3/2}}\right\} \tag{2}$$

The correspondence between the delta-Eddington phase function parameters and the Henyey-Greenstein phase function parameters is found by equating the first three moments of the Legendre polynomial expansion of each phase function. The result is[4]

$$f = (1-\beta)g_0^2 \qquad\qquad g' = \frac{g_0(1-g_0)}{\frac{1}{1-\beta}g_0^2} \tag{3}$$

The method used in this paper for obtaining the optical properties is similar to that used previously by Jacques and Prahl to measure the optical properties of albino mouse skin[5]. Basically, this involves obtaining an analytic solution to the radiative transport equation (simplified to a diffusion equation for the delta-Eddington phase function). The primary transmission measurement provides an estimate of the optical depth. The other two optical parameters (the albedo and the anisotropy) are then varied until the model predicts values for scattered transmittance and scattered reflectance that equal the measured values of scattered transmittance and scattered reflectance.

The phase functions above (equations 1 and 2) required two independent parameters. These two parameters combined with the unknown absorption and scattering yielded four unknowns. Because only three measurements were made, the four parameters could not be derermined uniquely. Instead results were found in terms of the transport scattering coefficient ($\mu_s'$) and the transport albed ($a'$). In the delta-Eddington approximation these are given by

$$\mu_s' = (1-f)\mu_s \qquad a' = \frac{\mu_s'}{\mu_s' + \mu_a} \qquad \tau' = d(\mu_s' + \mu_a) \tag{4}$$

where $\mu_s$ and $\mu_a$ are the scattering and absorption coefficients, and $d$ is the physical thickness of the sample.

Dimensionless optical properties were used. These are the transport albedo ($a'$), the optical depth ($\tau'$), and the delta-Eddington anistropy ($g'$). The use of dimensionless optical properties allowed optical properties to be obtained without the need for physical thickness information during aorta. The physical thickness, however, is necessary to extract values for the absorption and scattering coefficients from the dimensionless optical parameters.

The index of refraction was assumed to be constant, despite some evidence that the index of refraction of tissue varies with water content. This assumption was not too extreme since the estimated variation in the index of refraction (1.38 to 1.45) only changed the measured optical properties by 10%.

## RESULTS

The results of converting the measurements of reflectance and transmittance into optical properties ($a'$, $t'$, and $g'$) are shown in figure 3. The dashed lines indicate explosion and onset of charring times for the higher irradiance. The dotted lines do the same for the lower irradiance.

The most suprising finding is that there is very little change in the transport albedo until after the tissue explodes. At this time there is a slight decrease in the albedo corresponding to the onset of tissue boiling. After the onset of carbonization, the transport albedo drops sharply, indicating an increase in tissue absorption.

The initial drop in the anisotropy corresponds to tissue coagulation or blanching. This decrease indicates that the tissue scatters light more isotropically. Subsequent to the initial fall, the anisotropy increases linearly, corresponding to tissue dehydration and thinning. Thinning reduces the distance between scattering centers thereby increasing the effective size of the scatterers and, as in Mie scattering, the anisotropy as well.

The optical depth depends on the physical thickness of the sample (equation 4). This thickness is changing during irradiation due to tissue dehydration: if the absorption and scattering were constant, the optical depth would still change. The optical depth is quite sensitive to tissue coagulation and substatial changes occur in the first 50–75 seconds.

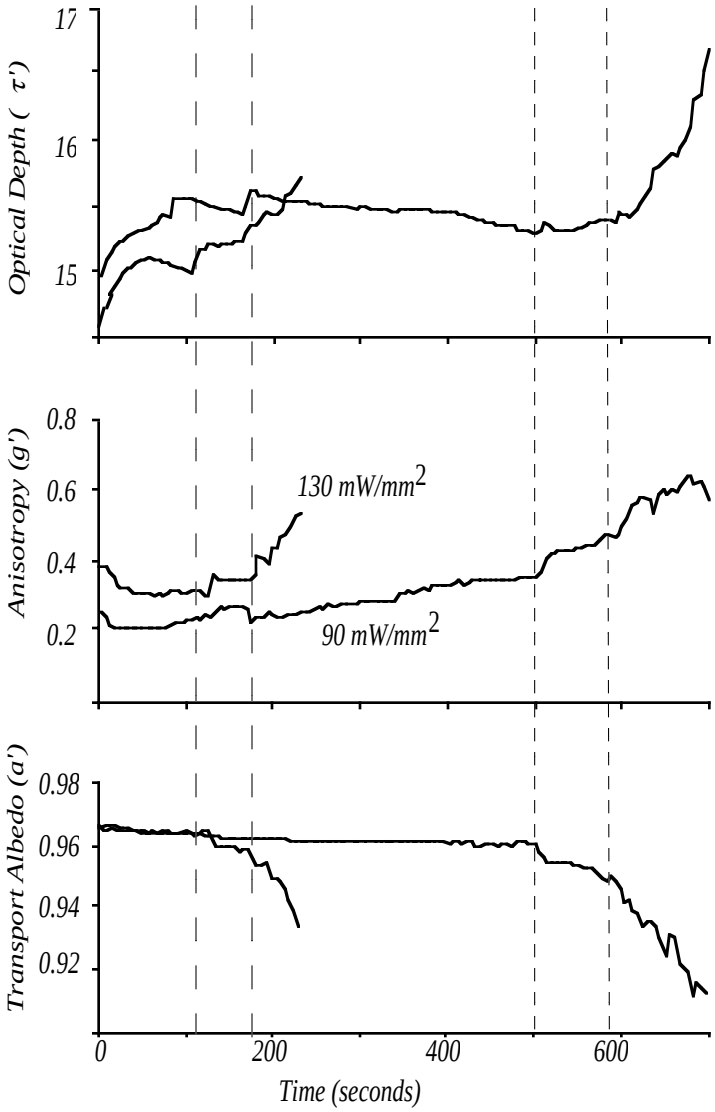


Figure 3: Optical properties of aorta.

## CONCLUSIONS

As expected the most drastic changes in optical properties are associated with charring: the albedo decreased and the delta-Eddington anisotropy ($g'$) increased. Unexpectedly, the effective albedo ($a'$) was relatively constant during coagulation and dehydration. These preliminary experiments illustrate a combined experimental and theoretical technique for measuring the optical properties of tissue during laser irradiation. Although the parameters presented are independent of tissue thickness, evaluation of absorption and scattering coefficients will require measurement of tissue thickness during irradiation.


## ACKNOWLEDGEMENTS

This research was partially supported by the Office of Naval Research under contract #N00014–86–K–0875.

## REFERENCES


[1] T. Halldórsson, W. Rother, J. Langerholc, and F. Frank, "Theoretical and experimental investigations prove Nd:YAG laser treatment to be safe," *Lasers Surg. Med.*, vol. 1, pp. 253–262, 1981.

[2] J. H. Joseph, W. J. Wiscombe, and J. A. Weinman, "The delta-Eddington approximation for radiative flux transfer," *J. Atmos. Sci.*, vol. 33, pp. 2452–2459, 1976.

[3] S. L. Jacques, C. A. Alter, and S. A. Prahl, "Angular dependence of HeNe laser light scattering by human dermis," *Lasers Life Sci.*, vol. 1, pp. 309–333, 1987.

[4] G. Yoon, A. J. Welch, M. Motamedi, and M. C. J. V. Gemert, "Development and application of three-dimensional light distribution model for laser irradiated tissue," *IEEE J. Quantum Electron.*, vol. QE-23, pp. 1721–1733, 1987.

[5] S. L. Jacques and S. A. Prahl, "Modeling optical and thermal distributions in tissue during laser irradiation," *Lasers Surg. Med.*, vol. 6, pp. 494–503, 1987.